17 p

Technical Report No. 32-555

Analysis Of Movable Louvers For Temperature Control

Joseph A. Plamondon

jpl
JET PROPULSION LABORATORY
CALIFORNIA INSTITUTE OF TECHNOLOGY
PASADENA, CALIFORNIA

January 1, 1964

Technical Report No. 32-555

Analysis Of Movable Louvers For Temperature Control

Joseph A. Plamondon

1 Jan. 1964 17 p refs

(NASA Contract NAS7-100)
(NASA CR-53046; JPL-TR-32-555)

OTS: $1.60 ph, $0.80 mf

Rob Roy McDonald

Rob R. McDonald, Jr., Chief
Engineering Research

12 DOTS

4742003

JET PROPULSION LABORATORY
CALIFORNIA INSTITUTE OF TECHNOLOGY
PASADENA, CALIFORNIA

January 1, 1964

Prepared Under Contract No. NAS 7-100
National Aeronautics & Space Administration

CONTENTS

FIGURES

ABSTRACT

14847

Movable shutters or louvers have been and will be employed on several spacecraft for active thermal control. The thermal performance of louvers, along with the controlling parameters, was analyzed, and seven equations describing the thermal behavior of a louver array were derived. Six of the equations, forming a simultaneous set consisting of three linear integral equations and three linear algebraic equations, describe the heat-transfer characteristics of an array. The seventh gives the relative thermal performance of an array in terms of effective emissivity. The equations are solved numerically, and effective emissivity is plotted as a function of louver blade position for various values of the dimensionless parameters that appear in the governing heat-transfer equations. The results are compared with experimental results obtained for the *Mariner* 2 spacecraft louver system. Author

I. INTRODUCTION

Providing a favorable thermal environment for the operation of electronic and mechanical equipment is a prime design objective in the development of a spacecraft. Thermal management or temperature control of a spacecraft is accomplished by creating a balance, within prescribed temperature tolerances, between the rates of heat absorption and heat rejection. For the most part, this balance is obtained by purely passive means; that is, the absorptivities of surfaces exposed to external heat sources and the emissivities of surfaces rejecting heat to space are selected to provide a balance of total heat input and output at acceptable temperatures. The purely passive approach to temperature control is perfectly admissible if all possible variations in the thermal environment of the spacecraft can be met with an invariant design in the sense that thermal parameters of the design cannot be varied in flight. As spacecraft become larger and more complex and as their missions become more encompassing, the need for active and positive control over the thermal parameters of a spacecraft while in flight will be required to meet gross changes in thermal environment, if the narrowing temperature tolerances imposed upon spacecraft systems are to be achieved.

In anticipation of future requirements for active temperature control, many schemes and devices have been proposed but few have been developed and actually flight tested. Among the active control systems successfully used aboard a space vehicle was that used on the *Mariner* 2 Venus fly-by. A *Mariner* type louver system consists of an array of movable blades having low emissivity surfaces and controlled thermostatically by bimetallic sensors which actuate the blades from a fully closed to a fully open position over a predetermined temperature range. Such an array is placed over a surface of relatively high emissivity to control the effective emissivity. When the array is closed, it acts as a

single radiation shield against the dissipation of heat from the high emissivity surface to space. As the blades open, the effective emissivity of the surface area increases as a result of an increasing view to space of the high emissivity surface. Thus, the blades essentially control the rate of radiative heat rejection to space.

Because louver systems have been successfully flown, and will undoubtedly be flown again, an analysis was undertaken to better understand the basic parameters which influence their thermal behavior. The purpose of this Report is to present the formulation and results of the analysis.

II. ASSUMPTIONS

As stated, the analysis was to determine the basic parameters and their influence on the gross thermal behavior of a louver array. Of particular interest is effective emissivity of an array as a function of louver blade opening angle as affected by surface properties (emissivity and reflectivity) and geometrical configuration (louver blade width to blade spacing). To this end, as many simplifying assumptions as possible are made without destroying those characteristics presumed to be intrinsic to the thermal behavior of an array, particularly with regard to the nonuniform temperature distribution on the louver blades and the nonuniform radiosity distribution on the blades and on the back surface (surface which the blades cover).

The assumptions made in the analysis are, in part, incorporated in the schematic or mathematical model used for the analysis, which is shown in Fig. 1. In the schematic model the coordinate axis x lies along the back surface, y lies along the inside of the louver blades, and z lies along the outside of the louver blades. It is necessary to distinguish between the inside and the outside of the blades because the radiosity (energy flux leaving) on one side is considerably different from that on the other side, as a result of having different geometrical views to each other, to the back surface, and to space. The louver blade opening angle is θ. When $\theta = 0$ deg the blades are in the closed position. The most significant simplifications result from the following assumptions:

1. The array is infinite in extent (to the right and left) and the blades are infinite in length (in and out of the paper).

2. All blades have the same angular position relative to the back surface.

3. The gap distance between the array and the back surface approaches zero.

4. Conduction in the blades in the y or z directions is negligible.

5. No temperature drop exists through the blades (normal to the y or z direction).

6. Emissivity of the blade surfaces is the same on both sides.

7. Temperature of the back surface is uniform.

8. The blades and the back surface emit and reflect diffusely.

The first three assumptions are made out of necessity since without them analysis would be formidable. The first and second assumptions force the thermal events within each channel, formed by two successive louver blades, to be identical by eliminating end-effects and by

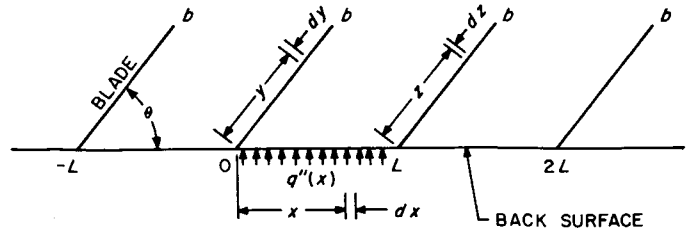

Fig.1. Mathematical model of louver array

making the configuration of each channel identical. The third assumption restricts interreflections between the back surface and the blades to one channel, since that portion of the back surface, between two successive blades, can only see the two blades. These three assumptions, therefore, reduce the analysis to a consideration of only one channel. The first assumption is fairly reasonable due to the construction of an actual finite array, at least from intuitive considerations: first, an array usually is made up of quite a few blades; second, a guard or sealing ring is placed around the array. The second assumption is reasonable if (1) all blades are actuated by a single actuator, or (2) adjacent actuators for individually actuated blades sense nearly the same actuating input. The third assumption somewhat distorts local heat transfer characteristics; however, the assumption has no effect on the over-all thermal characteristics of an array because in an infinite array the amount of energy escaping through the louvers is independent of the blades' pivotal position relative to the back surface.

The mathematical implications of the first three assumptions are enormous, resulting in a simplification of the problem from that of solving simultaneously several sets of simultaneous integro-differential equations (one set for each channel), with each equation having a large number of terms, to that of solving a single set of integro-differential equations, each having relatively few terms.

The fourth assumption reduces the set of integro-differential equations to linear integral equations, since it eliminates conduction from the analysis. This assumption along with assumption five is made on the basis of the *Mariner* 2 louver design, for which the blades were extremely thin, 0.005 in. thick. With such thin blades it is reasonable to conclude that conduction plays a minor role in the transfer process. Assumption five is reviewed in the final section of this Report. The sixth assumption results from current louver design practice. Assumptions five and six simplify the heat balance equation in the blades.

The seventh assumption arises from the fact that for many spacecraft, the surface to which a louver array is mounted is also a mounting surface for electronic components and, as such, is expected to carry some structural loads. As a result, the back surface is thick enough to produce reasonably uniform temperatures, even if the local radiant heat transfer rate to space varies considerably from location to location across the back surface.

Of the eight assumptions, the eighth is the most compromising and least valid. In the design of a louver system, the emissivity of the back surface is made as high as possible to give maximum control over heat dissipation through the array. It is also desirable to make the louver blades of a material that reflects energy specularly, which is, generally, the reflectance characteristic of low emissivity surfaces, especially when the energy spectrum is primarily in the infrared region. Specularly reflecting blades in the fully open or near fully open position tend to minimize the amount of energy leaving the back surface which returns to the back surface after an interaction with the blades. The advantageous effect of specularity decreases as the blades close. When the blades are completely closed specularity has no effect. To have made the analysis on the basis that the blades were specular rather than diffuse would have so seriously complicated the governing integral equations that a solution of the equations would not have been, in a practical sense, feasible at this time.

Along with the aforementioned eight assumptions, these generally accepted assumptions are listed: heat transfer to space is solely by radiation; space is at 0°R; all surfaces are gray reflectors and emitters; all material properties are constant; and no external sources of energy exist.

III. MATHEMATICAL FORMULATION

In deriving the heat transfer equations, the so-called radiosity approach is used (Ref. 1). From Fig. 1, it is obvious that symmetry does not exist, and, therefore, it is necessary to write a separate radiosity equation for each surface making up the channel. The differentials dx, dy, and dz (Fig. 1) represent differential areas on the back surface, inside blade surface, and outside blade surface, respectively. For convenience, the back surface is denoted by (1), the inside blade surface by (2), and the outside blade surface by (3). For each differential area radiant flux leaving points x on (1), y on (2), and z on (3) is denoted by $B(x)$, $C(y)$, and $D(z)$, respectively. Thus, B, C, or D represents the summation of the emitted energy and reflected energy leaving their respective differential areas. The emitted energy is given by the Stefan-Boltzmann law in the form $\epsilon\,\sigma\,T^4$, where σ is the Stefan-Boltzmann constant and ϵ is the gray-body hemispherical emissivity. The irradiance (incident energy) on dx, dy, and dz denoted by $H_1(x)$, $H_2(y)$, and $H_3(z)$ respectively, is expressed so that the reflected energy flux is given by $\rho\ H(\text{arg.}) = (1 - \alpha)\ H(\text{arg.})$, where α is the absorptivity. For gray bodies $\alpha = \epsilon$. With these definitions, the radiosity equation for each of the points, x, y, and z on surfaces (1), (2), and (3), respectively, can be written:

$$B(x) = \epsilon_1\,\sigma\,T_1^4 + \rho_1\,H_1(x) \tag{1}$$

$$C(y) = \epsilon_2\,\sigma\,T_2^4\,(y) + \rho_2\,H_2(y) \tag{2}$$

$$D(z) = \epsilon_2\,\sigma\,T_3^4\,(z) + \rho_2\,H_3(z) \tag{3}$$

The temperature T_1 is constant because of assumption six. The emissivities and reflectivities of surfaces (2) and (3) are equal because of assumption seven.

Since all surfaces are planar and, therefore, cannot see themselves and since no external sources of radiant energy exist, the irradiance on dx at x is, for example, composed of that portion of the flux leaving all points on (2) and all points on (3) and arriving at dx. Similarly, the irradiance on dy at y is composed of the flux leaving surfaces (1) and (3) and arriving at dy and similarly for the irradiance on dz at z. Since the irradiance on dx is composed of the total flux leaving surfaces (2) and (3), then $H_1(x)$ can be expressed in terms of $C(y)$ and $D(z)$. Since $C(y)$ is the energy flux leaving dy at y, then $C(y)dF_{y\text{-}x}$ is the flux leaving dy incident on dx when $dF_{y\text{-}x}$ is the geometrical view-factor of dx as seen from dy. By reciprocity, $dF_{y\text{-}x}\,dy = dF_{x\text{-}y}\,dx$; so, $C(y)dF_{y\text{-}x}\,dy = C(y)dF_{x\text{-}y}\,dx$. To obtain flux on dx divide out the dx, then total flux incident on dx from surface (2) is given by $\int_0^b C(y)dF_{x\text{-}y}$. Applying the same reasoning to obtain the total flux incident on dx at x from surface (3), and for the incident fluxes on dy and dz from the appropriate surfaces yields

$$H_1(x) = \int_0^b C(y)dF_{x\text{-}y} + \int_0^b D(z)dF_{x\text{-}z} \tag{4}$$

$$H_2(y) = \int_0^L B(x)dF_{y\text{-}x} + \int_0^b D(z)dF_{y\text{-}z} \tag{5}$$

$$H_3(z) = \int_0^L B(x)dF_{z\text{-}x} + \int_0^b C(y)dF_{z\text{-}y} \tag{6}$$

From Ref. 2, the two-dimensional incremental geometric view-factor is given by the simple expression

$$dF_{i\text{-}j} = \frac{1}{2}\,d(\sin\phi)$$

where ϕ is the angle formed by the outward normal from i and the radius vector from i to j. The expressions for the differential geometric view-factors are

$$dF_{x\text{-}y}\,dx = dF_{y\text{-}x}\,dy = \frac{xy\,(1 - \cos^2\theta)}{2(x^2 + y^2 - 2xy\cos\theta)^{3/2}}\,dx\,dy \tag{7}$$

$$dF_{x\text{-}z}\,dx = dF_{z\text{-}x}\,dz = \frac{z\,(L - x)\,(1 - \cos^2\theta)}{2\left[z^2 + (L - X)^2 + 2z\,(L - X)\cos\theta\right]^{3/2}}\,dx\,dz \tag{8}$$

$$dF_{y\text{-}z}\,dy = dF_{z\text{-}y}\,dz = \frac{L^2\,(1 - \cos^2\theta)}{2\left[(z - y)^2 + L^2 + 2\,(z - y)\,L\cos\theta\right]^{3/2}}\,dy\,dz \tag{9}$$

Substituting Eq. (4)-(9) into Eq. (1)-(3), gives

$$B(x) = \epsilon_1\,\sigma\,T_1^4 + (1 - \epsilon_1)\left(\int_0^b C(y)\,K_1(x,y)\,dy + \int_0^b D(z)\,K_2\,(x,z)\,dz\right) \tag{10}$$

$$C(y) = \epsilon_2\,\sigma\,T_2^4\,(z) + (1 - \epsilon_2)\left(\int_0^L B(x)\,K_1\,(x,y)\,dx + \int_0^b D(z)\,K_3\,(y,z)\,dz\right) \tag{11}$$

$$D(z) = \epsilon_2 \sigma T_3^4(z) + (1 - \epsilon_2)\left(\int_0^L B(x) K_2(x,z)\, dx + \int_0^b C(y) K_3(y,z)\, dy\right) \quad (12)$$

where

$$K_1(x,y) = \frac{xy(1 - \cos^2\theta)}{2\left[x^2 + y^2 - 2xy\cos\theta\right]^{3/2}} \quad (13)$$

$$K_2(x,z) = \frac{z(L-x)(1 - \cos^2\theta)}{2\left[(L-x)^2 + z^2 + 2z(L-x)\cos\theta\right]^{3/2}} \quad (14)$$

$$K_3(y,z) = \frac{L^2(1 - \cos^2\theta)}{2\left[(z-y)^2 + L^2 + 2(z-y)L\cos\theta\right]^{3/2}} \quad (15)$$

Eq. (13)-(15) are the kernels of the integral equations (Eq. 10-12).

Next, denoting the net energy flux dissipated at x from the back surface by $q''(x)$, where $q''(x)$ is the internal heat generation rate at x. This is related to the total energy dissipation rate at x by the expression

$$q''(x) = \epsilon_1 \sigma T_1^4 - \alpha_1 H_1(x) = \epsilon_1\left[\sigma T_1^4 - H_1(x)\right] \quad (16)$$

where $\epsilon_1 \sigma T_1^4$ is the emitted energy and $\alpha_1 H_1(x)$ is the absorbed irradiance.

Solving for $H_1(x)$ in Eq. (1) and substituting into Eq. (16) gives

$$q''(x) = \frac{\epsilon_1}{(1 - \epsilon_1)}\left[\sigma T_1^4 - B(x)\right] \quad (17)$$

Since energy is not generated internally in the louver blades, the equivalent of Eq. (16) for the location y or z on the blade is

$$\epsilon_2 \sigma T_2^4(y) + \epsilon_2 \sigma T_3^4(z) = \alpha_2 H_2(y) + \alpha_2 H_3(z) \quad (18)$$

when $y = z$. As a result of assumption five, $T_2(y) = T_3(z)$ when $y = z$. Solving Eq. (2) and (3) for $H_2(y)$ and $H_3(z)$, and substituting into Eq. (18), results in

$$2T_2^4(y) = 2T_3^4(z) = C(y) + D(z) \quad (19)$$

when $y = z$.

Investigating Eq. (10)-(12), (17), and (19) shows that the mathematical formulation of heat transfer through an array of louver blades from the back surface produces a set of six equations with six unknowns; namely, $B(x)$, $C(y)$, $D(z)$, $q''(x)$, $T_2(y)$ and $T_3(z)$. For convenience, the following is a regrouping of the six pertinent equations

$$B(x) = \epsilon_1 \sigma T_1^4 + (1 - \epsilon_1)\left(\int_0^b C(y) K_1(x,y)\, dy + \int_0^b D(z) K_2(x,z)\, dz\right) \quad (20)$$

$$C(y) = \epsilon_2 \sigma T_2^4(y) + (1 - \epsilon_2)\left(\int_0^L B(x) K_1(x,y)\, dx + \int_0^b D(z) K_3(y,z)\, dz\right) \quad (21)$$

$$D(z) = \epsilon_2 \sigma T_3^4(z) + (1 - \epsilon_2)\left(\int_0^L B(x) K_2(x,z)\, dx + \int_0^b C(y) K_3(y,z)\, dy\right) \quad (22)$$

$$2T_2^4(y) = C(y) + D(z)\ ,\ y = z \quad (23)$$

$$T_2(y) = T_3(z)\ ,\ y = z \quad (24)$$

$$q''(x) = \frac{\epsilon_1}{1 - \epsilon_1}\left[\sigma T_1^4 - B(x)\right] \quad (25)$$

Thus, the solution for the net heat transfer, $q''(x)$, through an array of louver blades requires the simultaneous solution of a set of six equations, three of which are integral equations.

As stated previously, the primary purpose of this analysis is to determine the effective emissivity of the array as a function of louver blade opening angle. To this end, let the effective emissivity of the array be defined as the ratio of net heat transfer from surface (1) to that amount of heat that would be dissipated if surface (1) were a black-body and louver blades did not interfere with the dissipation of heat; that is

$$\epsilon_T = \frac{\int_0^L q''(x)\, dx}{L \sigma T_1^4} \quad (26)$$

Thus, the effective emissivity is based on the back surface temperature. Clearly, this definition is independent of actuation techniques so long as the back surface temperature gradient is small between successive channels. Under the assumptions made, effective emissivity, as defined above, provides a useful and convenient tool for calculating the dissipation rate from a surface which is covered by an array of louver blades.

In order to write the above dimensional equations in dimensionless form let $x = \beta L$, $y = \zeta L$, and $z = \eta L$ and

substitute into Eq. (20)-(26); then divide all equations by σT_1^4, giving

$$B^*(\beta) = \epsilon_1 + (1 - \epsilon_1)\left(\int_0^{b/L} C^*(\zeta)\, K_1(\zeta, \beta)\, d\zeta + \int_0^{b/L} D^*(\eta)\, K_2(\eta, \beta)\, d\eta\right) \quad (27)$$

$$C^*(\zeta) = \epsilon_2\, T_2^*(\zeta) + (1 - \epsilon_2)\left(\int_0^{1.0} B^*(\beta)\, K_1(\zeta, \beta)\, d\beta + \int_0^{b/L} D^*(\eta)\, K_3(\zeta, \eta)\, d\eta\right) \quad (28)$$

$$D^*(\eta) = \epsilon_2\, T_3^*(\eta) + (1 - \epsilon_2)\left(\int_0^{1.0} B^*(\beta)\, K_2(\eta, \beta)\, d\beta + \int_0^{b/L} C^*(\zeta)\, K_3(\zeta, \eta)\, d\zeta\right) \quad (29)$$

$$q''^*(\beta) = \frac{\epsilon_1}{1 - \epsilon_1}\left[1 - B^*(\beta)\right] \quad (30)$$

$$2T_2^*(\zeta) = C^*(\zeta) + D^*(\eta) \quad , \quad \zeta = \eta \quad (31)$$

$$T_2^*(\zeta) = T_3^*(\eta) \quad , \quad \zeta = \eta \quad (32)$$

$$\epsilon_T = \int_0^{1.0} q''^*(\beta)\, d\beta \quad (33)$$

where

$$K_1(\zeta, \beta) = \frac{\beta\zeta\,(1 - \cos^2\theta)}{2\left[\beta^2 + \zeta^2 - 2\beta\zeta\cos\theta\right]^{3/2}} \quad (34)$$

$$K_2(\eta, \beta) = \frac{\eta\,(1 - \beta)\,(1 - \cos^2\theta)}{2\left[\eta^2 + (1 - \beta)^2 + 2\eta\,(1 - \beta)\cos\theta\right]^{3/2}} \quad (35)$$

$$K_3(\zeta, \eta) = \frac{(1 - \cos^2\theta)}{2\left[(\eta - \zeta)^2 + 1 + 2\,(\eta - \zeta)\cos\theta\right]^{3/2}} \quad (36)$$

An investigation of Eq. (27)-(36) reveals four independent dimensionless parameters which control the thermal behavior of an array: the blade opening angle θ; the emissivity of the back surface, ϵ_1; the emissivity of the louver blades, ϵ_2; and the ratio of louver blade width to louver blade spacing, b/L ($b/L \geqslant 1.0$). Therefore, the solution of these equations produces data which:

1. relates effective emissivity to blade opening angle
2. demonstrates the relative effects of back surface emissivity and blade emissivity on effective emissivity of the array
3. demonstrates the effect of the ratio of blade width to blade spacing on effective emissivity.

IV. SOLUTION

Because of the complexity of this set of simultaneous equations, solutions were obtained numerically using a digital computer. However, before numerical solutions could be undertaken, an investigation of the kernel functions revealed two problems: first, as the corners of the channel are approached (e.g., $\beta \to 0$ & $\zeta \to 0$ or $\beta \to 1$ & $\eta \to 0$) the kernel functions given by Eq. (34) and (35) become indeterminate; and second, when $\theta = 0$, the kernel function given by Eq. (34) becomes indeterminate at $\beta = \zeta$.

The indeterminate situation at the corners occurs regardless of how the corners are approached; that is, it makes no difference if the corners are approached from the center of the back-surface or downward along the blades. As a result, the kernel functions in all equations must be investigated. Consider first Eq. 27 as β approaches zero. To handle the indeterminate situation with $\beta = 0$ and $\zeta = 0$, make the following substitution (Ref. 3): let $\tau = \beta/\zeta$

$$\begin{aligned} &\text{at } \zeta = 0 \qquad \tau = \infty \\ &\text{at } \zeta = b/L \quad \tau = \beta\,(L/\beta) \end{aligned} \tag{37}$$

Substituting into Eq. (27) yields

$$B^*(\beta) = \epsilon_1 + (1-\epsilon_1)\left\{\int_{\beta(L/b)}^{\infty} C^*\left(\frac{\beta}{\tau}\right) \times \frac{(1-\cos^2\theta)}{2\left[\tau^2+1-2\tau\cos\theta\right]^{3/2}}\,d\tau + \int_0^{b/L} D^*(\eta)\,K_2(\eta,\beta)\,d\eta\right\} \tag{38}$$

and as $\beta \to 0$

$$B^*(0) = \epsilon_1 + (1-\epsilon_1)\left\{\int_0^{\infty} C^*(0) \times \frac{(1-\cos^2\theta)}{2\left[\tau^2+1-2\tau\cos\theta\right]^{3/2}}\,d\tau + \int_0^{b/L} D^*(\eta)\,K_2(\eta,0)\,d\eta\right\} \tag{39}$$

$C^*(0)$ is a constant and, as such, can be pulled out from under the integral; what remains can then be integrated. Equation (39) becomes

$$B^*(0) = \epsilon_1 + \frac{(1-\epsilon_1)}{2} \times (1+\cos\theta)\,C^*(0) + (1-\epsilon_1)\int_0^{b/L} D^*(\eta)\,K_2(\eta,0)\,d\eta \tag{40}$$

By the same procedure, as $\beta \to 1$ and $\eta \to 0$ Eq. (27) becomes

$$B^*(1) = \epsilon_1 + \frac{(1-\epsilon_1)(1-\cos\theta)}{2}\,D^*(0) + (1-\epsilon_1)\int_0^{b/L} C^*(\zeta)\,K_1(\zeta,0)\,d\zeta \tag{41}$$

As $\zeta \to$ & $\beta \to 1$ and $\eta \to 0$ & $\beta \to 1$ Eq. (28) and (29) become, respectively

$$C^*(0) = \epsilon_2\,T_2^*(0) + \frac{(1-\epsilon_2)(1+\cos\theta)}{2}\,B^*(0) + (1-\epsilon_2)\int_0^{b/L} D^*(\eta)\,K_3(0,\eta)\,d\eta \tag{42}$$

$$D^*(0) = \epsilon_2\,T_3^*(0) + \frac{(1-\epsilon_2)(1-\cos\theta)}{2}\,B^*(1) + (1-\epsilon_2)\int_0^{b/L} C^*(\zeta)\,K_3(0,\zeta)d\eta \tag{43}$$

When calculating the radiosities in the corners, these equations are substituted for Eq. (27)-(29).

Consider next the situation when the kernel given by Eq. (34) becomes indeterminate ($\theta = 0, \zeta = \beta$ for the case when $b/L = 1.0$). To handle this situation take the limit as θ approaches zero; Eq. (27) and (28) become, respectively

$$B^*(\beta) = \epsilon_1 + (1-\epsilon_1)\lim_{\theta\to 0}\int_0^{1.0} C^*(\zeta)\,K_1(\zeta,\beta)\,d\zeta \tag{44}$$

$$C^*(\zeta) = \epsilon_2\,T_2^*(\zeta) + (1-\epsilon_2)\lim_{\theta\to 0}\int_0^{1.0} B^*(\beta)\,K_1(\zeta,\beta)\,d\beta \tag{45}$$

In the above equations the integrals over surface (3) drop out. When $\theta = 0$, the back surface and the blades become parallel planes; and, because of assumption three,

they become, in effect, infinite parallel planes. Thus, from physical reasoning, the view of surface (1) from surface (2) or, conversely, the view of surface (2) from surface (1) becomes independent of location on either surface. Also the view of surface (3) to space becomes 1.0 and is independent of location on surface (3). Consequently, $B^*(\beta)$ and $C^*(\zeta)$ must be constants and Eq. (44) and (45) become

$$B^* = \epsilon_1 + (1 - \epsilon_1) C^* \lim_{\theta \to 0} \int_0^1 K_1(\zeta, \beta)\, d\zeta \quad (46)$$

$$C^* = \epsilon_2 T_2^* + (1 - \epsilon_1) B^* \lim_{\theta \to 0} \int_0^1 K_1(\zeta, \beta)\, d\beta \quad (47)$$

If the kernel function is first integrated and then the limit taken, it can be shown that

$$\lim_{\theta \to 0} \int_0^1 K_1(\zeta, \beta)\, d\zeta = \lim_{\theta \to 0} \int_0^1 K_1(\zeta, \beta)\, d\beta = 1 \quad (48)$$

Thus, for the case when $b/L = 1.0$, the transfer equations become

$$B^* = \epsilon_1 + (1 - \epsilon_1) C^* \quad (49)$$

$$C^* = \epsilon_2 T_2^* + (1 - \epsilon_2) B^* \quad (50)$$

$$D^* = \epsilon_3 T_3^* \quad (51)$$

$$2T_2^* = C^* + D^* \quad (52)$$

$$T_2^* = T_3^* \quad (53)$$

$$q''^* = \frac{\epsilon_1}{1 - \epsilon_1}(1 - B^*) \quad (54)$$

For the case when $b/L > 1.0$, the same procedure can be applied to the overlapped region, from $\zeta = 1$ to $\zeta = b/L$ and from $\eta = 0$ to $\eta = b/L - 1.0$, to determine the transfer relationships in the overlapped region of the blades.

To numerically solve Eq. (27)-(33), the power method was employed; an initial estimate was made for B^*, C^*, and D^* and the equations were integrated by Simpson's Rule. The new values of B^*, C^*, and D^* were then used in the next iteration. The process continued until convergence was achieved, which was assumed to have occurred when $q''^*(\beta)$ no longer changed in the third place.

The solutions of the equations were checked by equating the net radiant heat transfer from the back surface to the total radiosity that escapes directly to space from all surfaces.

$$\int_0^1 q''^*(\beta)\, d\beta = \int_0^1 B^*(\beta) M_1(\beta)\, d\beta + \int_0^{b/L} C^*(\zeta) M_2(\zeta)\, d\zeta + \int_0^{b/L} D^*(\eta) M_3(\eta)\, d\eta \quad (55)$$

The M's represent the form factors between the elemental areas $d\beta$, $d\zeta$, and $d\eta$, on surfaces (1), (2), and (3) and the open-end of the channel. Expressions for the M-terms are

$$M_1(\beta) = \frac{1 + \frac{b}{L}\cos\theta - \beta}{2\left[\left(1 + \frac{b}{L}\cos\theta - \beta\right)^2 + \left(\frac{b}{L}\sin\theta\right)^2\right]^{1/2}} + \frac{\beta - \frac{b}{L}\cos\theta}{2\left[\left(\beta - \frac{b}{L}\cos\theta\right)^2 + \left(\frac{b}{L}\sin\theta\right)^2\right]^{1/2}} \quad (56)$$

$$M_2(\zeta) = \frac{1}{2} - \frac{\frac{b}{L} - \zeta + \cos\theta}{2\left[\left(\frac{b}{L} - \zeta + \cos\theta\right)^2 + (\sin\theta)^2\right]^{1/2}} \quad (57)$$

$$M_3(\eta) = \frac{1}{2} - \frac{\frac{b}{L} - \eta - \cos\theta}{2\left[\left(\frac{b}{L} - \eta - \cos\theta\right)^2 + (\sin\theta)^2\right]^{1/2}} \quad (58)$$

V. RESULTS AND DISCUSSION

In obtaining numerical solutions, the primary purpose was to relate effective emissivity of an array to blade opening angle and to study the effect thereon of back-surface emissivity, blade emissivity, and the ratio of blade width to blade spacing. To this end solutions were obtained for θ over a range of 0 to 90 deg in increments of 5 or 10 deg for various values of ϵ_1, ϵ_2, and b/L. The number of values chosen for ϵ_1, ϵ_2, and b/L were limited from two to four values each, in order to economize machine time; therefore, only those values which bracket currently conceived areas of interest were chosen. IBM computers 7090 and 7094 were used to obtain the solutions.

Figure 2 is a plot of effective emissivity versus blade opening angle for various values of ϵ_1, with ϵ_2 and b/L constant. A quick calculation based on these results shows that the open value of effective emissivity is nearly a linear function of the back-surface emissivity, within 1.0 to 1.5% over the range considered. On the other hand, the closed value of effective emissivity is nearly independent of the back-surface emissivity. Of particular importance is the slope of the effective emissivity curve at small values of opening angle in the design of louver systems. Within the first 20 to 25 deg the effective emissivity changes by an order of magnitude from approximately 0.025 to 0.25 for small values of ϵ_2. Furthermore, within the first 2 deg the change is 100% or more. This indicates that, if reliance is placed upon the closed value of effective emissivity to achieve a thermal design objective, care must be taken to guarantee that the blades will close completely and that heat leaks at the ends of a finite array are sealed.

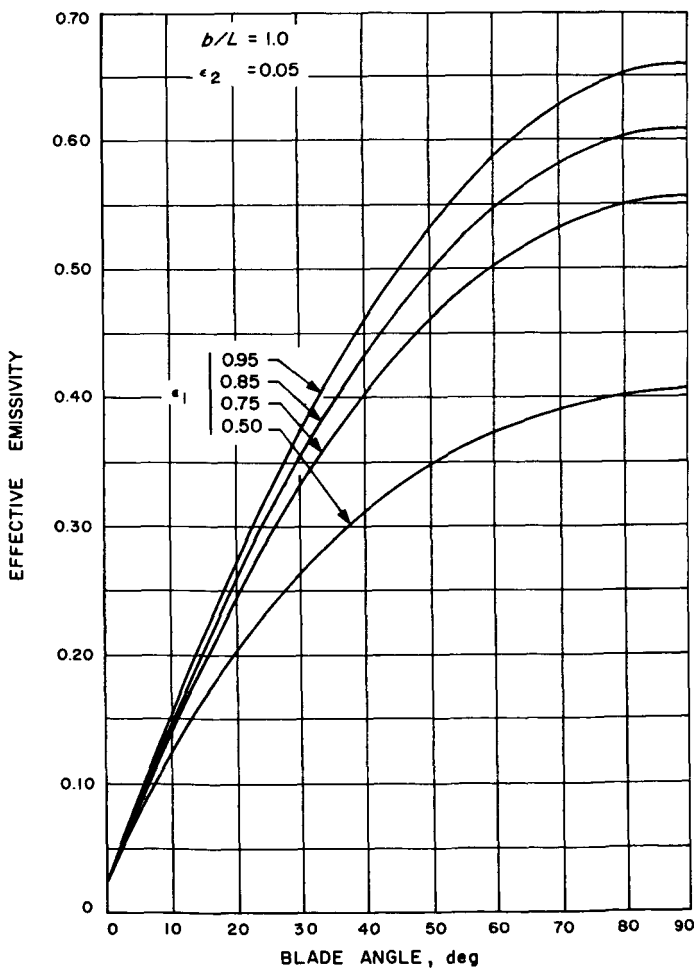

Fig. 2. Effective emissivity versus blade opening angle for various values of ϵ_1

Figure 3 is a plot of effective emissivity versus blade opening angle for various values of ϵ_2, with ϵ_1 and b/L constant. Clearly, large changes in ϵ_2 have negligible effect on the open value of effective emissivity. By way of explanation, if the temperature distributions on all surfaces making the channel were averaged and if effective emissivity calculations of an imaginary surface at the channel opening were based on this average temperature, it would be found that the channel acts nearly as a black cavity in relation to the average temperature. When the blades are closed the percent change in effective emissivity has nearly a 1:1 correspondence with the percent change in blade emissivity.

Figure 4 shows the effect of increasing b/L on effective emissivity. From these curves the advantage of overlapping the blades can be seen in that, if the blades overlap, complete closure of the blades is not so critical; however, the open value of effective emissivity does suffer somewhat.

Figures 5-7 show the distribution of local heat transfer from the back surface, the radiosity distribution of the blades, and the temperature distribution in the blades. These curves are plotted for a particular case of $\epsilon_1 = 0.95$, $\epsilon_2 = 0.05$, and $b/L = 1.0$. These plots indicate that it would be erroneous to assume that the radiosity distributions are uniform and that the local heat transfer rate is uniform. On the other hand, the rather large temperature gradients in the blades indicates, perhaps, that conduction in the blades should be taken into account,

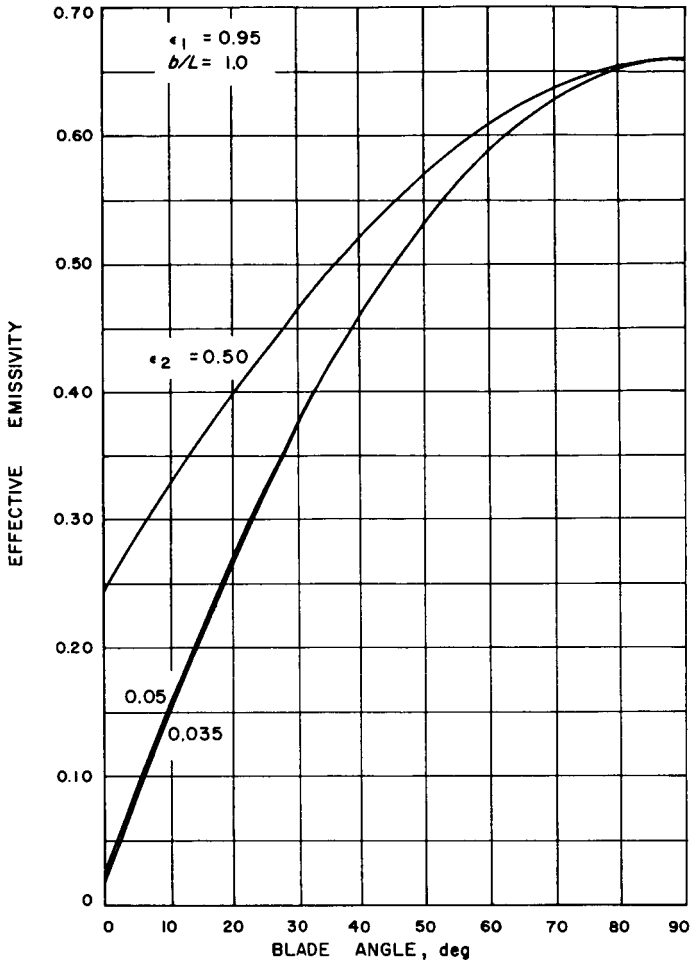

Fig. 3. Effective emissivity versus blade opening angle for various values of ϵ_2

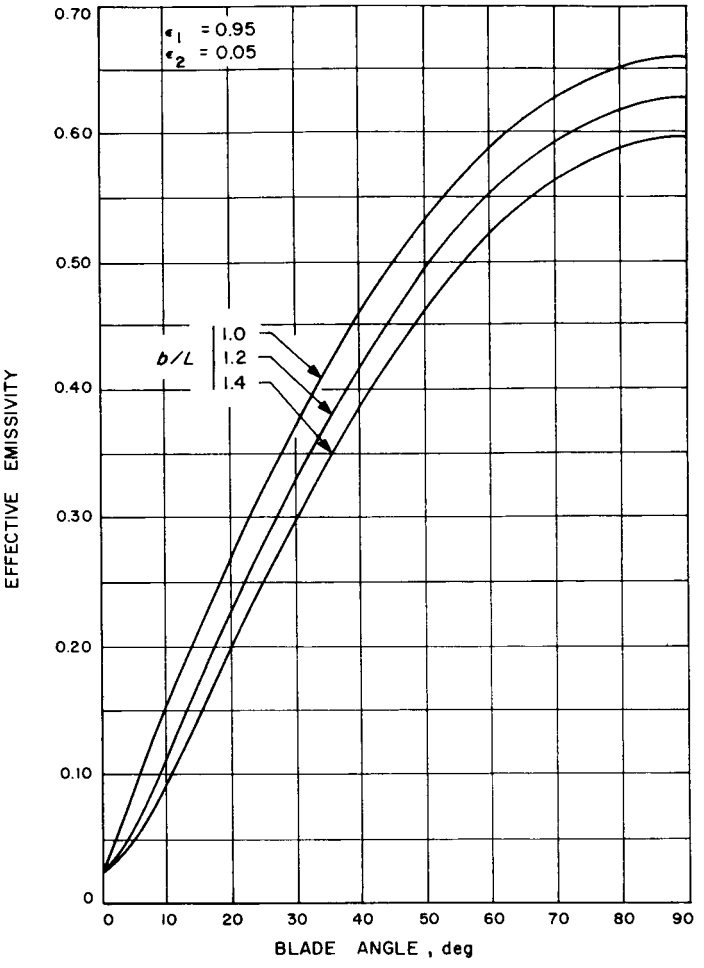

Fig. 4. Effective emissivity versus blade opening angle for various values of b/L

depending upon the material of the blades. If it is assumed that the blades are made of aluminum and their physical dimensions are of the order of 1.0 to 2.0 in. long and 0.005 in. thick, (Ref. 4) their efficiency as fins is quite good. This means that a uniform temperature for the blades would add complexity to the transfer equations in that blade temperature is an unknown and, therefore, computations would have to be based on the average amount of irradiance absorbed by the blades, which would remain nonuniform. This would inject another integral into the equations. It should be pointed out that the conduction in the blades would have negligible effect on the closed value of effective emissivity. In the open position conduction in the blades would tend to increase the value of effective emissivity, since the blade would act as a fin and transfer heat absorbed near the back surface to the tip where it could be more readily dissipated to space. If it is assumed that the blades are made from plastic, for example, the resulting fin efficiency is

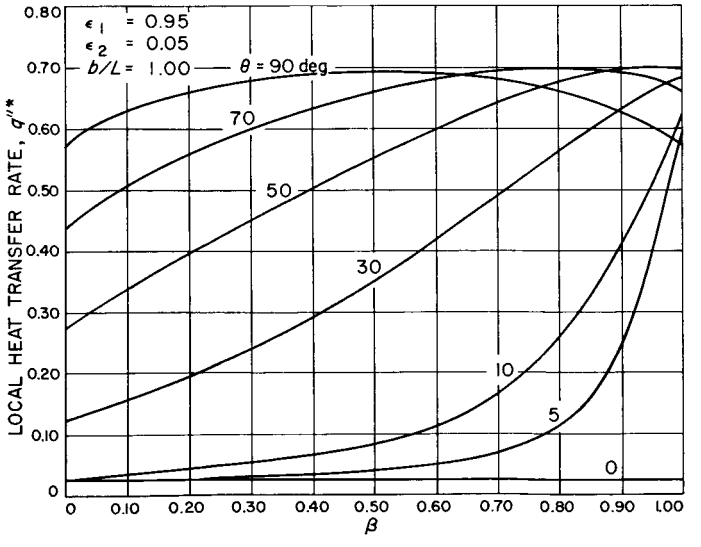

Fig. 5. Local heat transfer rate from back surface at various blade angles

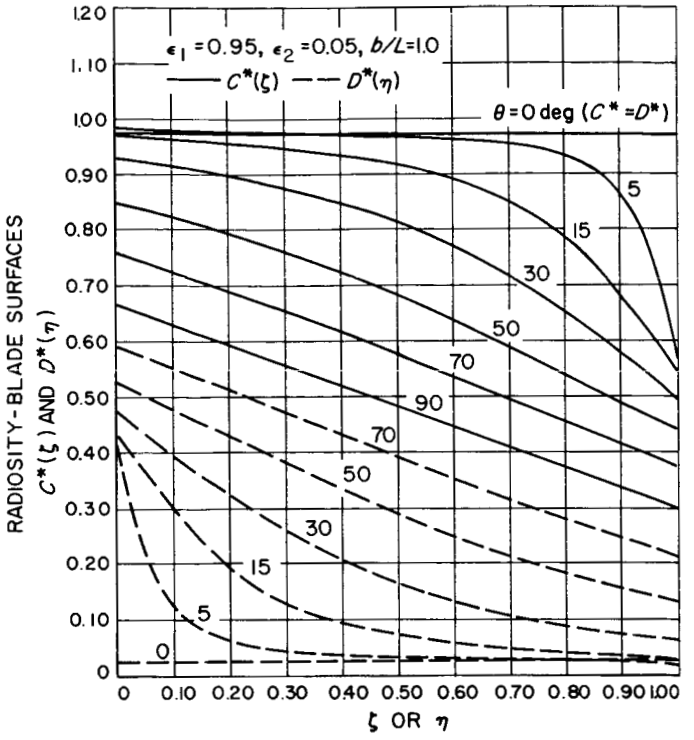

Fig. 6. Radiosity distributions along the blades at various blade angles

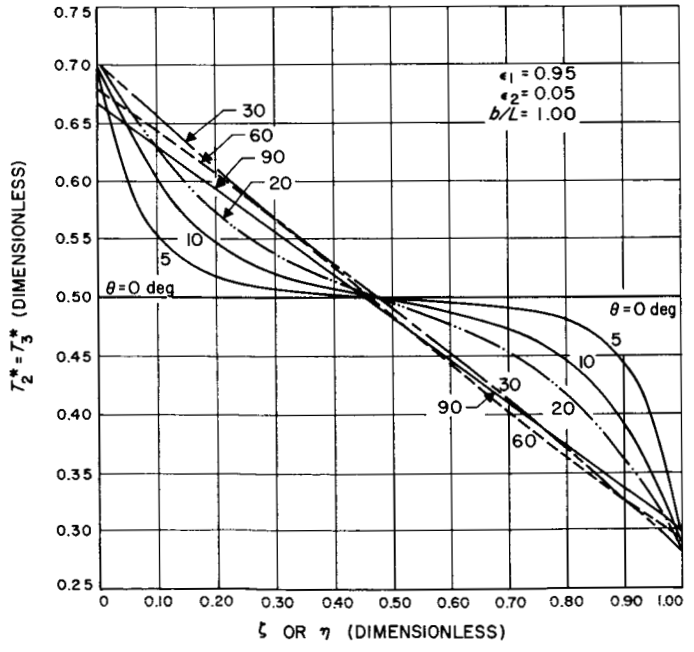

Fig. 7. Temperature distributions along the blades at various blade angles

quite low and the assumption made in this analysis is quite valid. In either case, by ignoring conduction in the blades, the closed value of effective emissivity is negligibly affected and the open value of effective emissivity predicted by the analysis is conservative, in the sense that the predicted value is lower than would be otherwise predicted. Consequently, the range of control as predicted by this analysis is less than it would actually be operationally, which for the thermal design engineer is conservative.

Finally, Fig. 8 is a comparison of predicted louver performance to experimental performance. The experimental data given in Fig. 8 is taken from the louver system used on the *Mariner* 2 spacecraft. The louver array used on the *Mariner* 2 covered an area of 1.28 ft² and was designed to open over the temperature range from 80 to 112°F. The actuation mechanisms were bimetallic springs having approximately a linear response to temperature; that is, θ was approximately linear with temperature. Figure 9 is a photograph of the *Mariner* 2 louver array, including the chassis or bay to which it was mounted.

The plot shown in Fig. 8 gives the temperature of the back surface as a function of the dissipated power. It should be made absolutely clear that for the test data the dissipated power is from the entire louver system,

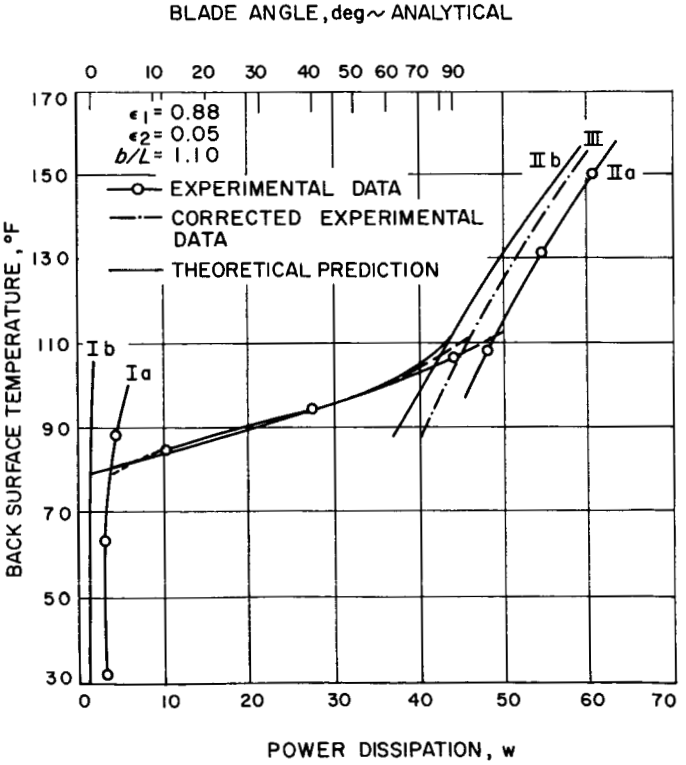

Fig. 8. Comparison of experimental and theoretical louver array performance

which includes all external hardware making the system. Thus, the power dissipated through the array of blades is somewhat less than the values indicated by the data; whereas, the predicted or analytical data in Fig. 8 is plotted only for power dissipated through an array of blades. Data for curves labeled Ia and Ib were obtained with the array caged in the closed position. The curves labeled IIa and IIb are for the louvers caged in the open position. The curves in between curves I and II show the operation of the louvers as they open or close.

In comparing the analytical with the experimental data, consider first the discrepancy between curves Ia and Ib. This discrepancy can be largely attributed to the fact that the experimental data includes dissipation from external hardware making up the system as well as dissipation through the array of blades. It can also be attributed, in part, to the fact that the test array is finite in size, and, therefore, heat losses must exist through gaps at the ends of the array. The discrepancy between curves IIa and IIb can also be attributed to the same factors plus an additional consideration; namely, the blades in the test array are specular in their reflective characteristics, whereas the analysis assumed the blades to be diffuse.

If the discrepancy between curves Ia and Ib is attributed to heat dissipation not passing through the array of blades but from associated hardware and end-effects and, further, if it is assumed that these losses are proportional to the fourth power of temperature, the experimental curves would move to the left when the discrepancy is corrected. Curve Ia moves to coincide with Ib and curve IIa becomes curve III, and by doing so the discrepancy between curves III and IIa is about 4.5%. By correcting the experimental data in the above manner, which is felt for the most part to be correct, the effect of specularity is about 4.5%. Thus, to assume that the blades are diffuse and, therefore, to take advantage of the resulting mathematical simplifications seems desirable.

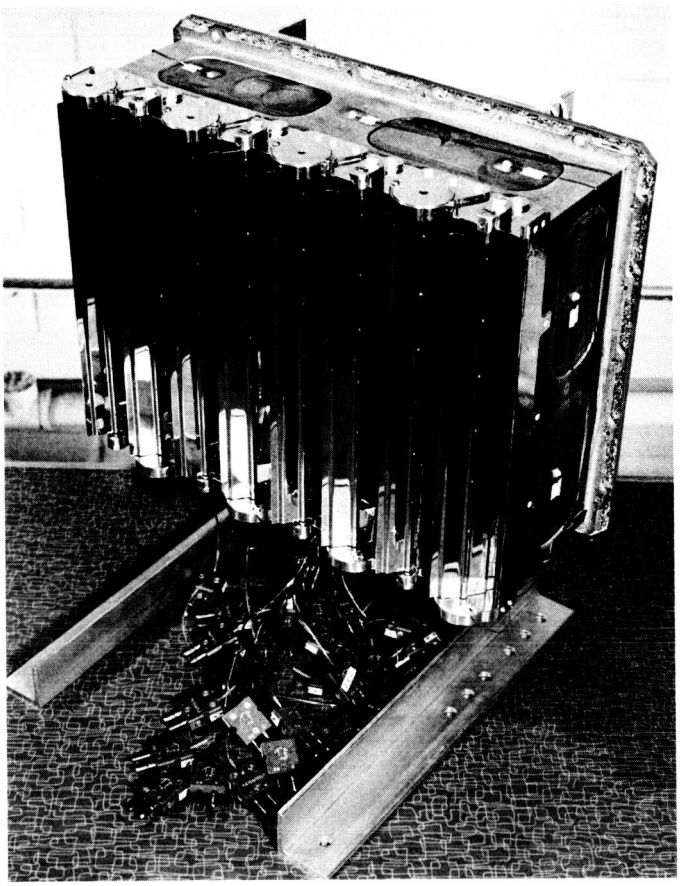

Fig. 9. Experimental test setup of the *Mariner* 2 louver system

ACKNOWLEDGMENT

We are grateful to Mr. Marshall Gram, of JPL, who kindly supplied the experimental data collected on the *Mariner 2* system and, also, to Mr. Ted Cullen, who programmed the equations for the numerical solution.

NOMENCLATURE

b	blade length (ft)
b/L	ratio of blade length to blade spacing
$B(x)$, $C(y)$, $D(z)$	local radiosity at x, y, and z, respectively (Btu/ft^2 hr)
$B^*(\beta)$, $C^*(\zeta)$, $D^*(\eta)$	local dimensionless radiosity at β, ζ, and η, respectively, $B(\beta)\,\sigma T_1^4$ $C(\zeta)/\sigma T_1^4$, and $D(\eta)/\sigma T_1^4$
dF_{i-j}	incremental view factor, from di *to* dj: where $i=x,y,z$; $j=x,y,z$; $i \neq j$
$H_1(x)$, $H_2(y)$, $H_3(z)$	local irradiance on dx, dy, and dz, respectively (Btu/ft^{2}hr)
$K(i,j)$	kernel function: $i=x,y,z$; $j=x,y,z$; $i \neq j$
L	blade spacing (ft)
$M_1(\beta)$, $M_2(\zeta)$, $M_3(\eta)$	view-factor from $d\beta$, $d\zeta$, and $d\eta$, to open end of channel, respectively
$q''(x)$	local heat transfer rate from back surface (Btu/ft^{2}hr)
$q''^*(x)$	dimensionless local heat transfer rate from back surface, $q''(\beta)/\sigma T_1^4$
$T_1(x)$, $T_2(y)$, $T_3(z)$	local temperature at x,y, and z ($^\circ R$)
$T_2^*(\zeta)$, $T_3(\eta)$	local dimensionless temperature to the fourth power at ζ and η, $\sigma T_2^4(\zeta)/\sigma T_1^4$, $\sigma T_3^4(\eta)/\sigma T_1^4$
x	coordinate along back surface (ft)
y, z	coordinates along inside and outside of blades (ft)
α_1	absorptivity of back surface
ρ_1, ρ_3	reflectivity of back surface and blade surfaces
ϵ_1, ϵ_2	emissivity of back surface and blade surfaces
ϵ_T	effective emissivity of louver array
β, ζ, η	dimensionless coordinates, x/L, y/L, z/L
θ	blade opening angle
σ	Stefan-Boltzmann constant

REFERENCES

1. Sparrow, E. M., J. L. Cregg, J. V. Szel, and P. Manos, "Analysis, Results, and Interpretation for Radiation Between Some Simply-Arranged Gray Surfaces," Transactions of the ASME, Series C, *Journal of Heat Transfer*, Vol. 83, 1961, pp. 207-214.
2. Jakob, Max, *Heat Transfer*, Vol. 2, John Wiley & Sons, Inc., New York, N. Y., 1957.
3. Heaslet, M. A., and H. Lomax, *Numerical Predictions of Radiative Interchange Between Conducting Fins with Mutual Irradiations*, National Aeronautical and Space Administration, Washington, D. C., 1961.
4. Plamondon, J. A., "Thermal Efficiency of Coated Fins," Transactions of the ASME, Series C, *Journal of Heat Transfer*, Vol. 84, 1962, pp. 279-284.